

Dosimetric Evaluation of Cardiac Structures on Left Breast Cancer Radiotherapy: Impact of Movement, Dose Calculation Algorithm and Treatment Technique

Esteban Barnafi Wittwer^{a, f}, Carolin Rippker^{b, f}, Paola Caprile^{c, g}, Demetrio Elias Torres^d, Rodrigo El Far^d, Araceli Gago-Arias^{c, e}, Tomas Merino^{a, d}

Abstract

Background: Breast cancer is the most frequently diagnosed and leading cause of cancer-related deaths among females. The treatment of breast cancer with radiotherapy, albeit effective, has been shown to be toxic to the heart, resulting in an elevated risk of cardiovascular disease and associated fatalities.

Methods: In this study, we evaluated the impact of respiratory movement, treatment plans and dose calculation algorithm on the dose delivered to the heart and its substructures during left breast radiotherapy over a cohort of 10 patients. We did this through three image sets, four different treatment plans and the employment of three algorithms on the same treatment plan. The dose parameters were then employed to estimate the impact on the 9-year excess cumulative risk for acute cardiac events by applying the model proposed by Darby.

Results: The left ventricle was the structure most irradiated. Due to the lack of four-dimensional computed tomography (4DCT), we used a set of images called phase-average CT that correspond to the average of the images from the respiratory cycle (exhale, exhale 50%, inhale, inhale 50%). When considering these images, nearly 10% of the heart received more than 5 Gy and doses were on average 27% higher when compared to free breathing images. Deep inspiration breath-hold plans reduced cardiac dose for nine out of 10 patients and reduced mean heart dose in about 50% when compared to reference plans. We also found that the implementation of deep inspiration breath-hold would reduce the relative lifetime risk

of ischemic heart disease to 10%, in comparison to 21% from the reference plan.

Conclusion: Our findings illustrate the importance of a more accurate determination of the dose and its consideration in cardiologists' consultation, a factor often overlooked during clinical examination. They also motivate the evaluation of the dose to the heart substructures to derive new heart dose constraints, and a more mindful and individualized clinical practice depending on the treatment employed.

Keywords: Cardiac dose; Left breast radiotherapy; Deep inspiration breath-hold; Risk of ischemic heart disease

Introduction

In 2019, heart disease and cancer were the leading causes of death worldwide [1]. As of 2021 [2, 3], breast cancer is the most frequently diagnosed cancer and leading cause for cancer deaths in females [4]. Radiotherapy (RT) is used as a complement to surgery (and chemotherapy) to reduce relapses and disease-related mortality [5]. Long-term patient survival has increased thanks to improvements in technology, and adverse effects related to the treatment, such as cardiovascular morbidity and mortality, are becoming increasingly relevant [6]. One systemic review assessed the risk of cardiovascular disease (CVD) in over a million women with breast cancer and found that CVD mortality is higher in breast cancer patients than in the general population, with 1.6% to 10.4% of all women with breast cancer dying of CVD [7].

Cardiovascular health and its risk factors were originally brought to light in the Framingham study [5], and continue to be essential in modern medicine, proving particularly important for breast cancer patients who are exposed to cardiotoxicity, a known side effect of RT. The relevance of cardiotoxicity in breast cancer RT is such that studies have quantified the relationship between ischemic heart disease (IHD) and mean heart dose (MHD) [8, 9]. Even though the mechanisms by which radiation induces heart disease are complex, nowadays they are better understood (Fig. 1) [8, 10-13]. Darby et al [8] found that for women treated with breast cancer RT, there is a linear correlation between heart dose and the rate of major

Manuscript submitted February 28, 2023, accepted May 5, 2023
Published online July 12, 2023

^aMedicine Faculty, Pontificia Universidad Catolica de Chile, Santiago, Chile

^bPhysics Faculty, Heidelberg University, Heidelberg, Germany

^cPhysics Institute, Pontificia Universidad Catolica de Chile, Santiago, Chile

^dCancer Center UC, Red de Salud Christus-UC, Santiago, Chile

^eGroup of Medical Physics and Biomathematics, Instituto de Investigacion Sanitaria de Santiago (IDIS), Santiago de Compostela, Spain

^fThese authors contributed equally to this work.

^gCorresponding Author: Paola Caprile, Physics Institute, Pontificia Universidad Catolica de Chile, Avda. Vicuna Mackenna 4860, Macul, Santiago, Chile. Email: pfcaprile@gmail.com

doi: <https://doi.org/10.14740/cr1486>

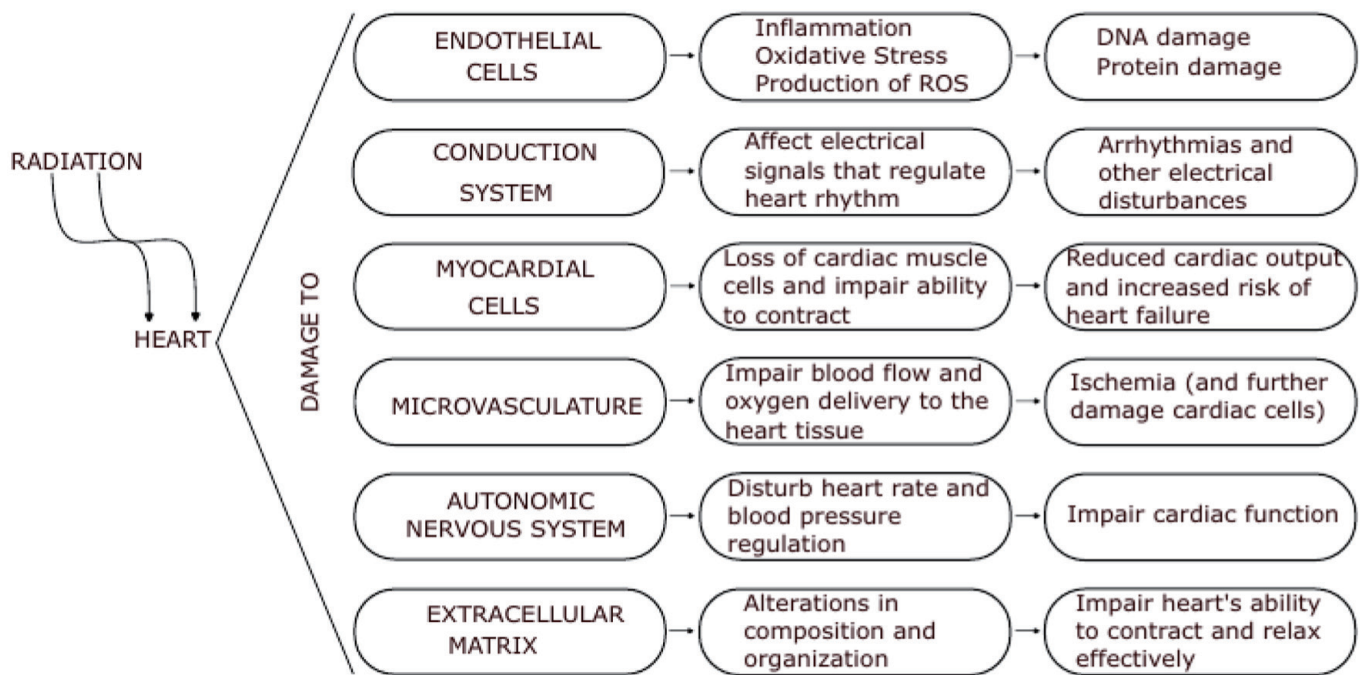


Figure 1. Effect of radiation on the heart. The physiopathology of radiation damage on the heart is complex and multifactorial, involving damage to the endothelial cells, conduction system, and myocardial cells themselves. The severity of radiation-induced cardiotoxicity depends on a variety of factors, including the dose and duration of radiation exposure, as well as individual patient factors such as age and underlying cardiovascular health.

cardiac events, with each Gray of MHD increasing the rate by 7.4%, with no apparent threshold. This has raised interest in cardiac surveillance and dose reduction to prevent cardiotoxicity and adverse outcomes.

Several strategies and studies have been published seeking to alleviate these problems and further our knowledge in regard to this matter, such as early detection of cardiac events [14, 15], evaluation of the dose to the substructures of the heart under different techniques of breast cancer RT [16-18], and the heart ischemic disease risk associated with the treatment [19, 20]. One such technique to reduce cardiac dose is moving the heart away from the breast during treatment with deep inspiration breath-hold (DIBH). A review of six studies evaluating the dosimetric impact of this technique for conformal radiation therapy reports MHD reductions ranging from 38% to 54% [21]. These findings are in agreement with previous works, which provide additional insights on the reduction of irradiated heart volume and other cardiac dose metrics [22-25].

However, despite previous approaches [13, 26], it remains unclear whether hot spots or MHD determine adverse cardiac effects. It has been suggested that certain areas of the heart might be more sensitive to radiation [27], such as the left anterior descending coronary artery (LAD), which is frequently included in the treatment field [28]. It has been also shown that the volume of the left ventricle within the treatment field predicts the development of short-term myocardial perfusion defects [29], and that the dose to upper substructures of the heart (atria and vessels) can be associated with non-cancer death [30, 31]. A study of lung cancer RT has also shown that doses

to specific heart substructures can be associated with different types of cardiac events, such as pericarditis, ischemia and arrhythmia [27]. This highlights the importance of contouring heart substructures to evaluate the dose distribution within the heart [28].

To the best of our knowledge, none of the prior studies evaluated the impact of intrafractional respiratory movement or the dose calculation algorithm employed on the cardiac substructures. Therefore, the objective of our work was to assess the effect of respiratory movement, treatment plans, and dose calculation algorithms on the dose to the heart and its substructures in a small cohort of patients undergoing left breast RT. Additionally, we aimed to investigate any changes in the ischemic risk associated with these scenarios.

Materials and Methods

We assessed RT dose distributions calculated for 10 patients with left breast carcinoma (Table 1). The purpose of this study was to analyze the effect of respiratory movement, treatment plans, and dose calculation algorithm on MHD. To accomplish this, we utilized three sets of images: free breathing (FB), DIBH, and a third set consisting of the average of images taken at four phases of the respiratory cycle (inhale, 50% inhale, 50% exhale and exhale) referred to as phase-average CT (paCT). Since a real four-dimensional computed tomography (4DCT) was not available at our institution, we defined the 4DCT image set for this study as the paCT.

Table 1. Cohort of Patients Along With Their Respective Medical History and Treatment Plan

	Patient 1	Patient 2	Patient 3	Patient 4	Patient 5	Patient 6	Patient 7	Patient 8	Patient 9	Patient 10
Age	45	42	75	49	59	43	69	63	67	61
Previous RT	No	No	Yes	No	No	No	No	No	No	Yes
Total Gy	52.5	50	40	40	40	40	40	40	42.5	66
Fractions	20	20	15	15	15	15	15	15	16	33
Boost	Yes	Yes	No	Yes						
Height (cm)	-	165	-	157	154	164	156	163	152	163
Weight (kg)	67	106	66	55	68	60	57	79.5	80	104
BMI	-	38.9	-	22.3	28.6	22.3	23.4	29.9	34.6	39.1
Smoker	Yes	Yes	Yes	Yes	Yes	No	Yes	Yes	No	Yes
DM2	No	Yes	No	No	Yes	No	No	Yes	No	No
AHT	No	No	No	No	Yes	No	Yes	No	Yes	No
DLP	No	Yes	No	No	No	No	No	Yes	No	Yes

AHT: arterial hypertension; BMI: body mass index; DLP: dyslipidemia; DM2: diabetes mellitus type 2; RT: radiotherapy.

Four treatment plans were generated and calculated for each patient. A base plan (BP) was generated and calculated on the FB image set, along with three other plans: generated on the FB set but calculated on the paCT image set (called from now on the reference plan), generated and calculated on the paCT image set (extended margin plan), and generated and calculated on DIBH (DIBH plan). The impact of dose calculation algorithm was assessed for pencil beam (PB), collapsed cone (CC), and Monte Carlo (MC) calculated dose distributions, only on the FB image set.

All participant patients were treated between July 2017 and May 2018 and gave written consent prior to their inclusion in the study. The study was conducted in accordance with a protocol approved by the ethics scientific committee of the Faculty of Medicine of Pontificia Universidad Catolica de Chile (CEC-Med UC), which adheres to the ICH GCP standards.

Before treatment, all patients underwent a planning kilovoltage CT (kVCT) scan with an axial slice thickness of 2 mm. The three sets of images were taken with the patients placed on a fixation board with the left arm above the head

and without contrast. Due to the use of paCT images and the risk of an allergic reaction to the contrast agent, we decided to limit the contouring to the heart and its four chambers (left ventricle (LV), right ventricle (RV), left atrium (LA) and right atrium (RA)), leaving aside arteries and other small cardiac substructures, which are difficult to differentiate unless images are cardiac-gated (Fig. 2). For consistency, all contours were delineated by the same physician following the guidelines of the cardiac atlas [32] and were supervised and approved by another radiation oncologist with more than 10 years of experience. Figure 2 shows an example of the set of images taken for one of the patients with contours of the target, heart and its four chambers.

Patients were treated on a Varian 6 MV linear accelerator (model 21Ex) with a field-in-field (FiF) technique, consisting of two opposing tangential 6 MV beams using dynamic wedges. If needed, additional fields were added as a boost to improve target dose homogeneity depending on patient anatomy. BPs were simulated using the FB CT image set to define the fields and generate the dose distributions. Dose calculations were performed with an Eclipse version 8.6 (Varian Medi-

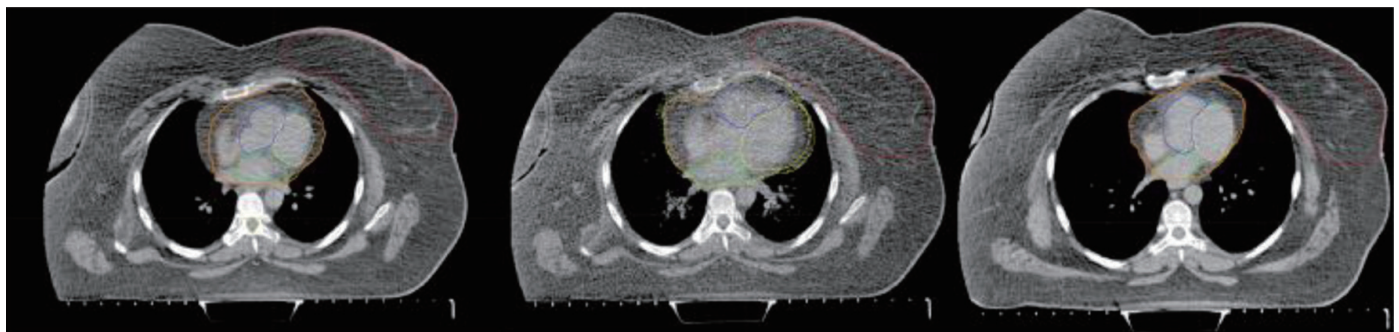


Figure 2. Example of the set of images acquired for one patient: free breathing CT (left); paCT (middle); and DIBH CT (right). Red contours correspond to the target, while yellow, blue, green and orange contoured substructures in the heart correspond to left and right ventricles and left and right atria, respectively. Blurred heart and cardiac substructures can be seen in the central image due to movement. CT: computed tomography; DIBH: deep inspiration breath-hold; paCT: phase-average CT.

cal Systems, Palo Alto, CA, USA) treatment planning system (TPS) using a PB convolution algorithm. The planning target volume (PTV) prescribed dose was either 50 Gy (in 25 fractions), 42.5 Gy (in 16 fractions), or 40 Gy (in 15 fractions) to the whole breast, complemented by a boost of 10 Gy in three cases. In one patient who underwent mastectomy before treatment, the chest wall was treated. The plan MHD constraint was 3 Gy, which increased to 5 Gy when the internal mammary node was also treated.

The dosimetric parameters for the heart that were recorded for each patient and treatment plan included mean dose, minimum dose to the 20 most irradiated cubic centimeters of volume (D_{20cc}), the volumes that receive 2/5 Gy or more ($V2/V5$), and dose volume histograms (DVHs). The contoured substructure volume variations due to movement were also assessed. Parameter values for the whole heart and its substructures were compared with those registered in the BP. Boxplots were used to represent parameter differences, with stars indicating outliers (beyond $1.5 \times$ interquartile range) and whiskers extending to the most extreme data values that are not outliers. The statistical significance of the observed differences was assessed using the non-parametric Wilcoxon signed rank test.

Respiratory movement

To quantify the impact of respiratory movement during irradiation on the dose to the heart, the patient's dose distributions were recalculated using the paCT image sets for the same plan previously defined. This enabled us to account for involuntary respiratory motion and obtain a more accurate assessment of the dose received by the different structures during treatment delivery, which was originally planned using the FB CT image.

Motion management

As previously mentioned, in order to evaluate the impact of motion management techniques on cardiac dose, we conducted simulations of three additional treatment plans for each patient. These plans included: 1) Reference plan: This plan was generated using the FB CT scan but calculated on the paCT image set. This approach allowed us to assess the dose delivered to the different organs when accounting for movement, providing a more accurate estimation of the dose delivered to the patients. 2) Extended margin plan: This plan was generated and calculated using the paCT image set, enabling identification of the range of respiratory movement of both the target and heart as contoured structures. 3) DIBH plan: This plan was generated and calculated using the DIBH image set, which increases the distance between the target and the heart.

Algorithms

Eclipse and Monaco are both TPSs used for radiation therapy. Eclipse is developed by Varian Medical Systems, while Monaco is developed by Elekta. They use different algorithms

(such as PB, MC or CC) to calculate the dose distribution in the patient's body, and each has different modeling capabilities. They both have inherent differences such as the way they model the treatment beam. In this study, both Eclipse and Monaco were used to generate treatment plans and calculate MHD for each patient.

It is well known that commercial TPS dose calculation algorithms may exhibit poor performance when it comes to computing out-of-field dose distributions [33]. To investigate this issue, we conducted a comparison of the peripheral cardiac dose derived from the BP, which employed the PB algorithm of Eclipse, with the dose from equivalent plans calculated with CC and MC, implemented in Monaco version 6.0 (Elekta CMS, Maryland Heights, MO, USA). These plans were replanned using CC and MC in Monaco and are not the same plan as the one using PB in Eclipse. We generated equivalent plans, where equal nominal energy beams, number of fields, and target dose homogeneity were employed, along with coverage of at least 95% of the target's volume with the same prescribed dose, resulting in an equivalent dose distribution.

To perform the comparison, we utilized the FB CT image sets to simulate new plans in Monaco for all patients. Only these image sets were considered in order to isolate the impact of the algorithm from the effect of respiratory movement. Dose distribution calculations were conducted using the three algorithms available: PB, CC, and MC. DVH and mean dose to the target, heart, and its substructures were exported in each case for comparison, using MC calculations as reference.

IHD risk

The dose parameters associated with the analyzed scenarios were then employed to estimate the impact on the 9-year excess cumulative risk for acute cardiac events by applying the model proposed by Darby et al [8].

Results

Unless otherwise specified, all differences in the values of dosimetric parameters related to the heart and its substructures were found to be significant at a 0.05 significance level using the Wilcoxon test.

Table 2 illustrates the mean values of volume, dose and D_{20cc} of the heart and its substructures on FB CTs, along with the relative increase in cardiac volumes due to movement. The analysis of the contoured substructure volume variations resulting from movement indicated that the paCT images yielded larger structures. For most cardiac substructures, significant increments (averaging more than 20%) were observed.

Figure 3 demonstrates the differences in cardiac dose observed after recalculating the plans on the paCT images. The modified dose distributions provide a more realistic estimation of the expected dose to the different structures during treatment delivery. It is worth noting that the MHD increased on paCT compared to FB CT calculated plans, despite larger volumes. The LV had the largest average mean dose variation

Table 2. Volume and Dose Parameter Values (Mean Dose and D_{20cc}) for the Heart and Its Substructures on FB and Volume Increments due to Movement

	FB CT volume (cc)	FB CT mean dose (cGy)	FB CT D_{20cc} (cGy)	paCT volume increment (%)
Heart	679 ± 46	236 ± 29	1,650 ± 430	19.9 ± 8.1
LV	171.4 ± 3.9	381 ± 64	830 ± 200	35 ± 11
RV	106.0 ± 6.8	256 ± 57	293 ± 56	36 ± 14
LA	78 ± 13	74.2 ± 3.3	82.3 ± 4.4	0.8 ± 6.4
RA	67.7 ± 6.2	65.6 ± 3.7	70.1 ± 3.2	42 ± 14

CT: computed tomography; FB: free breathing; LA: left atrium; LV: left ventricle; RA: right atrium; RV: right ventricle; paCT: phase-average CT.

due to movement among the substructures. For the right substructures, mean dose differences in both scenarios were not significant. Although large variations in D_{20cc} were observed due to movement, only differences for the heart and RA were significant due to the large variability of this parameter value between patients (Fig. 3, right).

Comparison of the dose-volume metrics presented in Table 3 demonstrated that significant parts of the heart, accounting for $9.1 \pm 1.3\%$ of the volume, received more than 5 Gy when considering paCT images. It can be observed that except for the RA, V2, and V5, all heart substructures' volumes increased for the paCT images when compared to the FB CTs. Differences diminished when considering volume in percent, as the larger contoured volumes on the paCT images contributed to the increase in V2/V5. However, differences in the LV were not statistically significant.

As expected, DIBH images indicated a displacement of the heart with respect to the target due to the increased lung

volume. On average, patients' left lung volumes were $74 \pm 16\%$ larger for this technique than when measured on FB.

In Figure 4, we compare mean dose and D_{20cc} on the investigated structures for DIBH with respect to the reference plan. The mean dose was reduced on DIBH plans for all the evaluated substructures, with the LV experiencing the most significant reduction. A reduction trend was also observed for all the structures regarding the D_{20cc} parameter. In this case, the relative variation was even larger than for the mean dose. Consistently, D_{20cc} values for the left lung changed marginally ($-2.1 \pm 1.5\%$) with respect to the reference plan, as part of this structure always remains close to the target.

Figure 5 depicts that switching from the reference to the extended margin technique also leads to a notable reduction in heart dose. However, the dose reduction observed in DIBH was greater than that achieved with the extended margin plan. The extended margin plan decreased mean doses to the heart and LV by $23.1 \pm 4.1\%$ and $26.0 \pm 3.5\%$, respectively, while DIBH

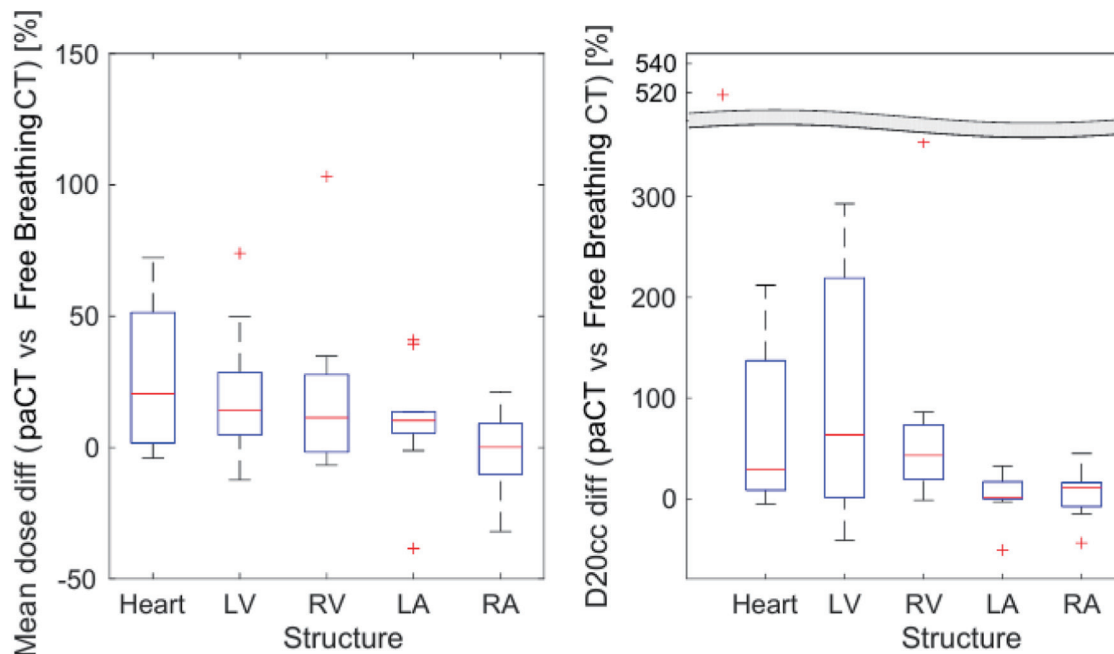
**Figure 3.** Difference between patients' doses calculated using paCT and FB CT images. Mean dose (left) and D_{20cc} (right) for each structure. CT: computed tomography; D_{20cc} : minimum dose to the 20 most irradiated cubic centimeters of volume; FB: free breathing; paCT: phase-average CT.

Table 3. Comparison of V2 and V5 Values Calculated on FB CT and paCT Image Sets for the Reference Plan

			Heart	LV	RV	LA
FB CT	V2	(cc)	129 ± 17	61.2 ± 7.8	29.5 ± 5.8	0.14 ± 0.11
		(%)	18.9 ± 2.0	36.0 ± 4.8	27.1 ± 4.9	0.22 ± 0.18
	V5	(cc)	46.0 ± 7.6	23.2 ± 4.1	7.8 ± 2.9	0 ± 0
		(%)	6.8 ± 1.0	13.7 ± 2.5	7.1 ± 2.6	0 ± 0
paCT	V2	(cc)	180 ± 25	85 ± 13	40.0 ± 6.0	2.1 ± 1.1
		(%)	22.0 ± 2.3	36.5 ± 4.7	29.3 ± 4.0	3.0 ± 1.5
	V5	(cc)	75 ± 12	37.1 ± 7.1	13.0 ± 4.0	0.24 ± 0.16
		(%)	9.1 ± 1.3	15.8 ± 2.7	9.2 ± 2.6	0.32 ± 0.22

As reference, parameter values are also shown as a percentage of the corresponding substructure volume. Right atrium's parameters were excluded from this table as all values were equal to zero within uncertainties. CT: computed tomography; FB: free breathing; LA: left atrium; LV: left ventricle; RV: right ventricle; paCT: phase-average CT.

lowered the mean doses to the heart and LV by 43.3±7.0% and 49.2±6.9%, respectively. Similarly, though the D_{20cc} parameter saw a dose reduction with the extended margin technique, this reduction was smaller than that observed for the DIBH technique.

Table 4 displays that in the patient cohort, the volumes of cardiac substructures that received doses higher than 2 or 5 Gy were significantly reduced with the DIBH technique compared to the reference plan. V5 values for both ventricles and the whole heart were reduced on average by more than 50%, while there were no significant differences for V2 and V5 of the atria. The table also shows that considering respiratory movement during the planning simulation led to a reduction in V2 and V5 for the extended margin plan compared to the reference plan. Although all structures had systematically reduced mean values, the Wilcoxon test did not find significant

variations for the atria.

Figure 6 provides an example of the DVH for the heart and substructures for one patient calculated for the same plan with different algorithms. Although minor differences were observed between CC and MC, doses were significantly lower when calculated using PB. As mentioned earlier, the LV is located closer to the field, and it is therefore the most irradiated cardiac substructure. The three algorithms produced target doses that agreed within 2%, as seen in Table 5, with PB calculations showing a greater underestimation. Figure 7 compares the mean dose to different organs and substructures calculated with PB and CC to MC.

In our patient group, this implementation of PB underestimated the MHD by 15.4±2.8% compared to MC. For the heart's larger sub volumes, i.e., the LV and RV, PB underestimated doses by 10.1±2.6% and 16.3±4.1%, respectively, which was

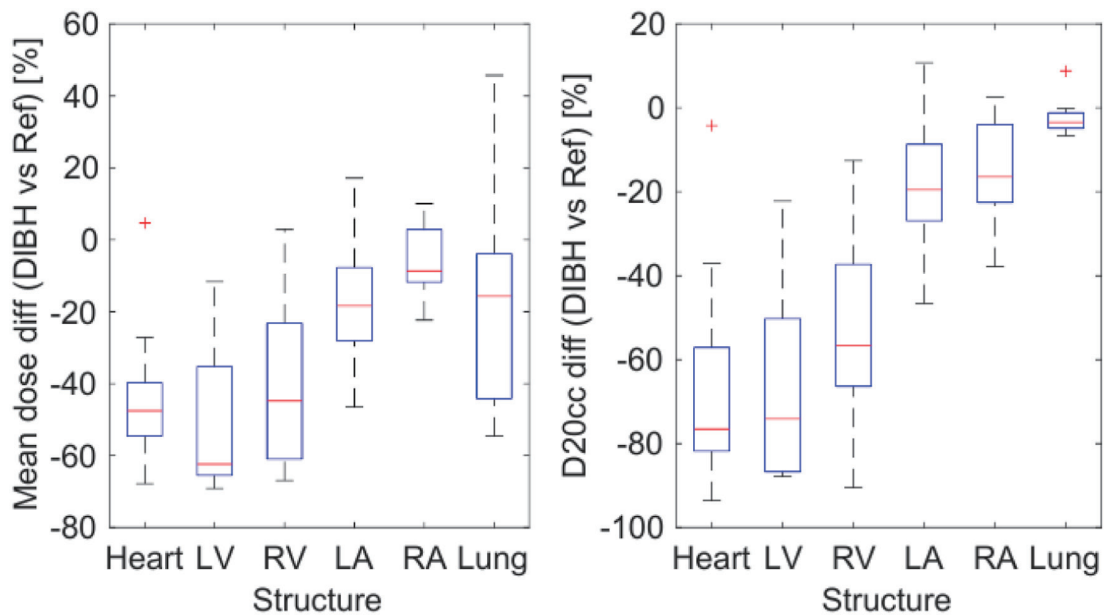


Figure 4. Difference of mean dose (left) and D_{20cc} (right) on each structure for the 10 patients, calculated for the DIBH plan vs. the reference plan. DIBH: deep inspiration breath-hold; D_{20cc}: minimum dose to the 20 most irradiated cubic centimeters of volume.

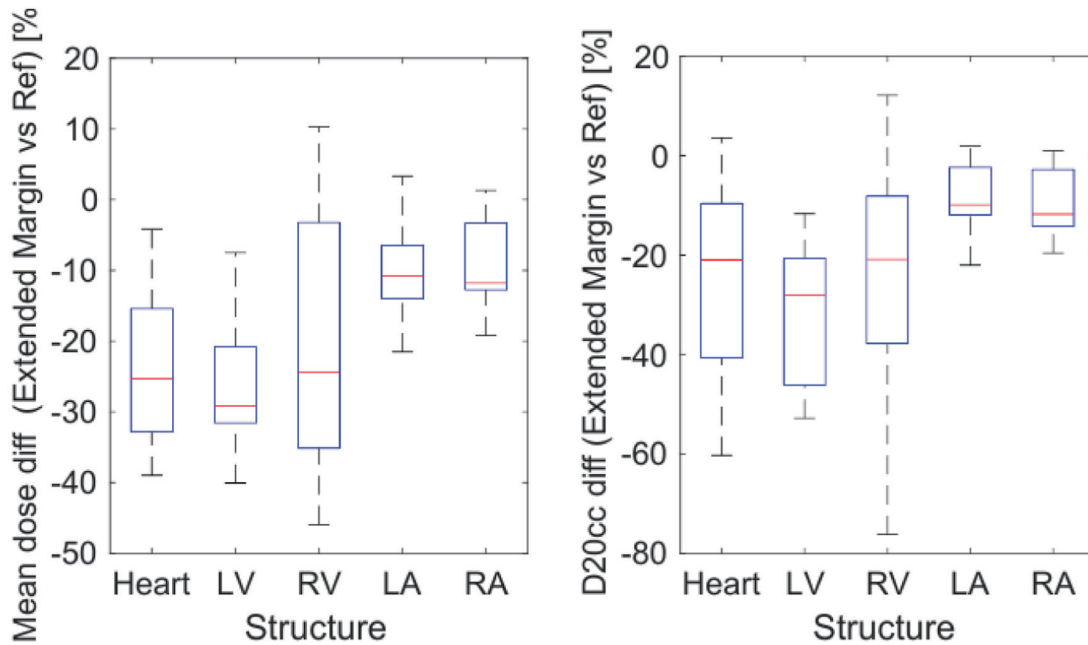


Figure 5. Difference of mean dose (left) and D_{20cc} (right) on each structure for the 10 patients, calculated for the extended margin plan vs. the reference plan. D_{20cc} : minimum dose to the 20 most irradiated cubic centimeters of volume.

similar to the observed MHD underestimation. Conversely, for smaller structures such as the LA and RA, PB underestimated the mean dose by about 90%. CC overestimated doses by below 2.5% for the heart and ventricles, and these differences were not significant as per the Wilcoxon test. In the atria, an overestimation of approximately 20% was noted. As expected, the relative difference increased as cardiac substructures were further away from the treatment field.

Using Darby’s linear dependence between mean heart equivalent dose in 2 Gy fractions (EQD2) and IHD risk [8],

the relative increase in lifetime risk can be estimated from the calculated patient dose distributions. Table 6 displays the mean EQD2 values and the associated relative risk increments for the different treatment scenarios examined. The reference plan, which we recall is generated in FB but calculated in paCT, takes into account respiratory movement. In contrast, the BP assumes a static position by being generated and calculated in FB. The use of the reference plan is associated with an increase of 40.8% in the relative risk of ischemic disease. However, the extended margin plan, which is a plan generated and calculated

Table 4. Comparison of V2 and V5 Values for the Reference, Extended Margin and DIBH Plans

			Heart	LV	RV	LA
Reference	V2	(cc)	180 ± 25	85 ± 13	40.0 ± 6.0	2.1 ± 1.1
		(%)	22.0 ± 2.3	36.5 ± 4.7	29.3 ± 4.0	3.0 ± 1.5
	V5	(cc)	75 ± 12	37.1 ± 7.1	13.0 ± 4.0	0.24 ± 0.16
		(%)	9.1 ± 1.3	15.8 ± 2.7	9.2 ± 2.6	0.32 ± 0.22
Extended margin	V2	(cc)	152 ± 26	73 ± 13	31.4 ± 7.1	1.44 ± 0.73
		(%)	18.1 ± 2.6	30.8 ± 4.7	21.9 ± 4.3	2.0 ± 1.0
	V5	(cc)	59 ± 13	29.2 ± 6.6	8.9 ± 4.0	0.104 ± 0.074
		(%)	6.9 ± 1.4	12.1 ± 2.6	5.8 ± 2.5	0.14 ± 0.10
DIBH	V2	(cc)	98 ± 24	44 ± 10	15.7 ± 5.2	0.27 ± 0.19
		(%)	14.8 ± 3.5	24.8 ± 5.5	17.1 ± 5.5	0.62 ± 0.48
	V5	(cc)	27.9 ± 8.3	12.4 ± 3.9	2.5 ± 1.4	0 ± 0
		(%)	4.2 ± 1.2	7.0 ± 2.0	2.5 ± 1.4	0 ± 0

As reference, parameter values as a percentage of the corresponding substructure volume are also shown. Right atrium’s parameters were excluded from this table as all values were equal to zero within uncertainties. DIBH: deep inspiration breath-hold; LA: left atrium; LV: left ventricle; RV: right ventricle.

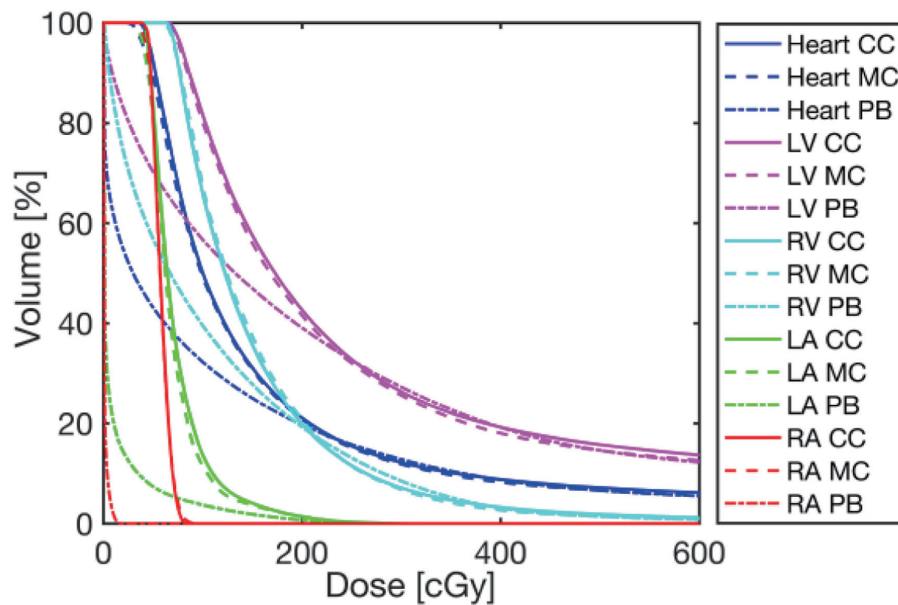


Figure 6. Representative DVH of one patient for the heart and cardiac substructures calculated with the three algorithms: PB, CC and MC. DVHs for the target, heart and its substructures. CC: collapsed cone; DVH: dose volume histogram; MC: Monte Carlo; PB: pencil beam.

using paCT, reduces the relative risk from the reference plan by 29.1%. The DIBH plan further reduces the relative risk of ischemic disease to a total of 53.1%.

Van den Bogaard [9] has proposed a model that validates and complements Darby’s [8] linear estimation based on MHD. In addition to MHD, Van den Bogaard’s model also takes into account substructure dose parameters (LV’s V5) and clinical risk factors such as age, diabetes, hypertension, and previous ischemic cardiac events to estimate the risk. Although Van den Bogaard’s model is an improvement over Darby’s, it was not used in this study due to the lack of medical history from the patients, particularly information on previous IHD, which is essential for calculating their linear predictor.

Discussion

The acquisition of FB CT images on a random phase of the cardiac and respiratory cycle allowed for easy differentiation of heart substructures, such as ventricles and atria. However, on paCT images, identifying heart substructures is often chal-

Table 5. Mean Dose to the Target Calculated With the Different Algorithms, and Their Difference in Percentage in Respect to MC

	Mean dose to the target (cGy)	Comparison to MC (%)
MC	4558,67	0
PB	4490,21	-1,35
CC	4565,27	0,21

CC: collapsed cone; MC: Monte Carlo; PB: pencil beam.

lenging due to the addition of image sets resulting in a blurred image that shows all cardiac substructures overlapping, as shown in Figure 2.

As our institution did not have access to a real 4DCT, the 4DCT image set was defined in this study as the average of images taken at the four respiratory phases. This may have led to an overestimation of the impact of movement, as it displayed the extreme case where the patient remains in full in and exhale as long as in intermediate phases.

Improvement of delineation of heart substructures could be achieved through the use of contrast [34], making it possible to assess doses to smaller heart substructures such as the LAD. Alternatively, structures could be contoured on each image phase, where they are more clearly visible, and interpolated. However, this would significantly increase the workflow time of the process. In a recent study by Guzvha et al, substructure volume variations due to respiratory movement were assessed for mediastinal lymphoma and lung cancer [34]. Changes with respect to a 50% respiratory phase were calculated. Our changes in the ventricles’ volumes were larger than in this work (35% vs. 14.5% and 36% vs. 19%, for the LV and RV respectively), but discrepancies between both works can be explained due to the use of different methodologies and observers.

As the LV is closest to the treatment field, the dose to this structure is the most affected by respiratory motion. In contrast, right and left atria, which are far from the field in left breast cancer FiF treatment, undergo no significant dose changes. On average, significant portions of the heart (nearly 10%) received more than 5 Gy when considering paCT images. Considering that the cardiac dose may be underestimated by PB, this could lead to cardiac dose constraints being exceeded.

This study evaluated two alternative treatment techniques

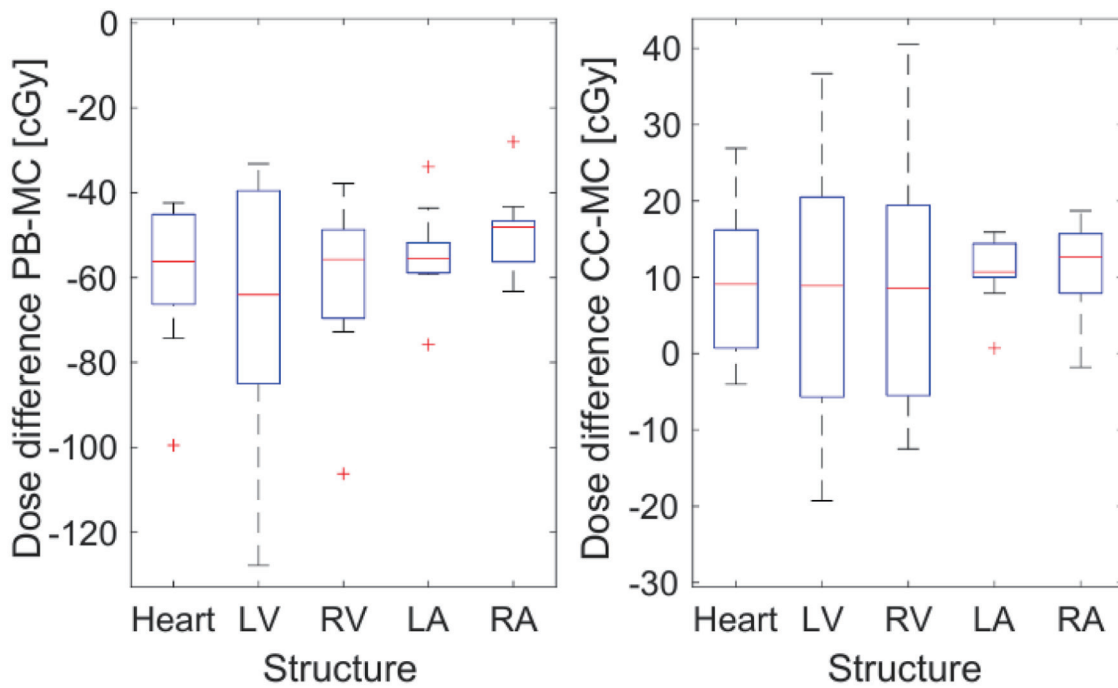


Figure 7. Mean difference in cGy between patient mean doses calculated for different structures with PB, CC and MC in Monaco. The dose calculated with Monte Carlo is used as a reference. CC: collapsed cone; MC: Monte Carlo; PB: pencil beam.

to FiF treatment planned on a FB CT image. DIBH plans allowed for a reduction in cardiac dose for all patients included in the study, except for one case where the distance from the heart to the breast was not enlarged during inspiration due to the patient’s anatomy. On average, patients received significantly smaller mean doses to the heart and LV, with smaller D_{20cc} values for these structures. Again, dose changes were larger for the ventricles, which are closer to the treatment field. Tang et al [18] observed that the substructures receiving the largest doses remained unchanged between techniques (DIBH and FB), without accounting for respiratory movement. We found these findings to be true even when considering the effect of respiratory movement. This was expected given the orientation of the fields and the principal direction of the res-

Table 6. Mean EQD2 and Mean Relative Increase of Ischemic Heart Disease Risk Corresponding to the Dosimetric Scenarios Analyzed: Conventional (Reference) Treatment Calculated on FB CT or paCT, Extended Margin and DIBH Plans

	Mean EQD2 (Gy)	Relative risk increment (%)
Base plan (FB CT)	1.75 ± 0.30	14.7 ± 2.5
Reference (paCT)	2.46 ± 0.43	20.7 ± 3.6
Extended margin	1.88 ± 0.37	15.8 ± 3.1
DIBH	1.17 ± 0.24	9.8 ± 2.0

The reported risk uncertainties only consider dose variations within the cohort. CT: computed tomography; DIBH: deep inspiration breath-hold; EQD2: equivalent dose in 2 Gy fractions; FB: free breathing; paCT: phase-average CT.

piratory heart movement [34]. Additionally, the sparing of the heart (relative mean dose reduction) estimated in our work for the implementation of DIBH was consistent with the results shown in previous studies [25, 35].

Regarding relative IHD risk, Eldredge-Hindy et al [19] calculated lifetime risk variations in DIBH and FB treatments for different baseline risk populations. For their overall cohort, the mean EQD2 reduction with DIBH was more drastic than in our case. Although they did not take into account respiratory heart movement, our results lie within their reported ranges. Considering movement, we also found a drastic (more than 50%) change in the relative risk between DIBH and the reference plan.

Dose calculation algorithms provided by commercial TPS are intended to perform accurate dose distribution calculations in the region where the upper 50% of the dose is delivered [33]. For left breast RT, dose underestimation in the heart is therefore expected due to the lack of good modeling of peripheral dose. Previous works have shown that PB does not account properly for the contribution of scattering outside of the treatment field [36]. In our study, this effect led to an important underestimation of cardiac dose, while the target dose remained comparable within 2% with respect to MC calculations performed by Monaco, which are considered the gold standard for this work. Dose values registered in the patients’ heart substructures are in agreement with previous studies reporting that PB dose underestimation is smaller for the heart structures lying closer to the treatment field, i.e., LV dose is more precisely calculated than other substructures [33]. Discrepancies between CC and MC were much smaller, with CC overestimations of about 2.5% observed for the heart and the

ventricles, while larger deviations were obtained for the atria.

Since Darby et al's [8] estimation of ischemic risk is based on TPS dose calculations, where no information is provided about the specific algorithm used for planning, we did not correct our risk estimations for these effects. Assuming that a PB algorithm may have been used in this work, our estimations should be consistent. Nevertheless, it is important to note that the algorithm chosen for the calculation would have an important impact on the cardiac risk estimation.

Our main objective in constructing this manuscript was to evaluate the impact of the mentioned variables on the calculated dose to the heart and its substructures, but other interesting and applicable results have also emerged from this work. Firstly, and most importantly, the findings of this work can be used by clinicians in limited-resource scenarios to personalize radiation therapy plans for patients with breast cancer and select the most appropriate treatment technique. Additionally, this same information can be used to improve treatment planning strategies and optimize treatment outcomes for patients with breast cancer.

Our results can serve as a guide for clinical decision-making in patients undergoing radiation therapy, as well as for patients who have already finished their treatment plans. In the latter case, clinicians can use this information to adjust their future treatment plans based on the dose and algorithms used in their radiation plans.

The limitations of this work include, but are not limited to, a small cohort of patients, the use of a technique (FiF) that is not universally employed and may therefore reduce the scope of the study's applicability, the unavailability of breath control, the inability to apply Van den Bogaard's model due to the lack of IHD history in the cohort, the consideration of a large number of variables per patient in a small cohort, and as previously mentioned, Eclipse and Monaco have inherent differences which could potentially affect the accuracy of the MHD calculation but further studies are needed to evaluate the impact of the choice of TPS on MHD. Additionally, the available technology does not yet permit accurate calculation of dose distribution in the area below 50% of the prescribed dose, which renders PB unsuitable for estimating relative ischemic heart risk due to the increasing discrepancy between PB and CC/MC as one moves further from the target, as our findings indicate.

As such, this study could be further improved by using a larger and more homogeneous cohort, employing real 4DCT, implementing breathing control, obtaining more detailed medical histories from the patients, reducing the number of variables considered, utilizing the same TPS for every plan, and utilizing technology that can identify smaller cardiac substructures.

Another way to improve this study is by using an automated approach that would allow us to expand our sample size and apply our procedures. RT processes are currently being studied and validated for automation and the use of artificial intelligence. However, this field of research is yet to be validated for clinical use, and there is a lack of confidence with regards to the application and clinical use of artificial intelligence, including medical-legal responsibility. In our case, artificial intelligence was not used due to its unavailability and it still being an area of research.

Regarding the use of 4DCT, if it had been available, the results regarding the assessment of dose to the heart and substructures during treatment considering movement would have been even more realistic, as it would have allowed for a more detailed evaluation of respiratory movement. Nevertheless, as we considered the complete range of heart motion during respiration for the assessment, a small impact on the variation of dose distribution to the heart and its substructures is expected. Our findings are consistent with previous studies that have utilized 4DCT, suggesting that the overall conclusions of the study are robust.

Conclusion

In this study, we assessed dose parameters in heart substructures while taking into account respiratory movement, different treatment techniques, and dose calculation algorithms. Our results showed that the mean cardiac dose was on average $27\pm 12\%$ higher when calculated on paCT images than when estimated in FB CTs. DIBH plans were observed to reduce MHD by approximately 50% compared with the reference plan in our cohort. Alternatively, extended margin plans were observed to reduce cardiac dose by 23%. On the LV, which was the most irradiated heart substructure, dose variations were even greater.

Considering the aforementioned effects, it was possible to evaluate the changes in the relative IHD risk increment due to treatment. For the reference plan, the estimated relative cardiac disease risk increment due to treatment was approximately 21%. The implementation of DIBH would reduce this relative risk to approximately 10%, while the value for the extended margin plan would be 16%. These findings suggest that DIBH and extended margin plans could be used to reduce the risk of IHD in patients undergoing radiation therapy.

Despite the progress proposed in this study, several open challenges remain regarding MHD calculations. The accurate estimation of peripheral cardiac dose and the use of smaller heart substructures, such as LAD instead of the traditional four chambers, are two significant obstacles that must still be overcome.

Nevertheless, our findings contribute to the current state of knowledge in the field and provide valuable information on the assessment of MHD in settings where top of the line technology is not yet available.

This, as mentioned before, can be used to inform personalized treatment plans for patients. Clinicians must be aware of the ischemic heart risk and its accuracy, allowing them to make informed decisions and establish a personalized course of action in relation to the patient's cardiovascular health. Further research is needed to build on these findings and improve the accuracy of MHD calculations in clinical settings.

Overall, our study highlights the importance of taking into account respiratory movement and the impact of different treatment techniques and dose calculation algorithms on heart substructures. We hope that our findings will contribute to the development of more personalized and effective radiation therapy plans for patients, ultimately improving their overall health outcomes.

Acknowledgments

None to declare.

Financial Disclosure

This project was funded by FONDECYT Iniciacion 2017: 11170575.

Conflict of Interest

None to declare.

Informed Consent

The authors certify that all participant patients gave written consent prior to their inclusion in the study.

Author Contributions

CR and AGA designed and performed the study. TM established plans and acquired consent. PC, CR, DET and REF calculated the different plans. EBW drafted this manuscript and did critical editing. TM and PC supervised the preparation and writing of this manuscript.

Data Availability

The authors declare that all data supporting the findings of this work are available within the article.

Abbreviations

AHT: arterial hypertension; BMI: body mass index; BP: base plan; CC: collapsed cone; CT: computed tomography; CVD: cardiovascular disease; DIBH: deep inspiration breath-hold; DLP: dyslipidemia; DM2: diabetes mellitus type 2; D_{20cc} : minimum dose to the 20 most irradiated cubic centimeters of volume; DVH: dose volume histogram; EQD2: equivalent dose in 2 Gy fractions; FB: free breathing; FiF: field-in-field; IHD: ischemic heart disease; LA: left atrium; LAD: left anterior descending coronary artery; LV: left ventricle; MC: Monte Carlo; MHD: mean heart dose; paCT: phase-average CT; PB: pencil beam; PTV: planning target volume; RA: right atrium; RT: radiotherapy; RV: right ventricle; TPS: treatment planning system; V2: volume that receives 2 Gy or more; V5: volume that receives 5 Gy or more

References

- Ritchie H, Spooner F, Roser M. Causes of death. Our World in Data 2018. <https://ourworldindata.org/causes-of-death>.
- Giaquinto AN, Miller KD, Tossas KY, Winn RA, Jemal A, Siegel RL. Cancer statistics for African American/Black People 2022. *CA Cancer J Clin.* 2022;72(3):202-229. [doi pubmed](#)
- Miller KD, Ortiz AP, Pinheiro PS, Bandi P, Minihan A, Fuchs HE, Martinez Tyson D, et al. Cancer statistics for the US Hispanic/Latino population, 2021. *CA Cancer J Clin.* 2021;71(6):466-487. [doi pubmed](#)
- Torre LA, Islami F, Siegel RL, Ward EM, Jemal A. Global cancer in women: burden and trends. *Cancer Epidemiol Biomarkers Prev.* 2017;26(4):444-457. [doi pubmed](#)
- Ebctcg, McGale P, Taylor C, Correa C, Cutter D, Duane F, Ewertz M, et al. Effect of radiotherapy after mastectomy and axillary surgery on 10-year recurrence and 20-year breast cancer mortality: meta-analysis of individual patient data for 8135 women in 22 randomised trials. *Lancet.* 2014;383(9935):2127-2135. [doi pubmed pmc](#)
- Bloom MW, Hamo CE, Cardinale D, Ky B, Nohria A, Baer L, et al. Cancer therapy-related cardiac dysfunction and heart failure. *Circulation: Heart Failure* 2016;9(1):2661. [doi](#)
- Gernaat SAM, Ho PJ, Rijnberg N, Emaus MJ, Baak LM, Hartman M, Grobbee DE, et al. Risk of death from cardiovascular disease following breast cancer: a systematic review. *Breast Cancer Res Treat.* 2017;164(3):537-555. [doi pubmed pmc](#)
- Darby SC, Ewertz M, McGale P, Bennet AM, Blom-Goldman U, Bronnum D, Correa C, et al. Risk of ischemic heart disease in women after radiotherapy for breast cancer. *N Engl J Med.* 2013;368(11):987-998. [doi pubmed](#)
- van den Bogaard VA, Ta BD, van der Schaaf A, Bouma AB, Middag AM, Bantema-Joppe EJ, van Dijk LV, et al. Validation and modification of a prediction model for acute cardiac events in patients with breast cancer treated with radiotherapy based on three-dimensional dose distributions to cardiac substructures. *J Clin Oncol.* 2017;35(11):1171-1178. [doi pubmed pmc](#)
- Wang H, Wei J, Zheng Q, Meng L, Xin Y, Yin X, Jiang X. Radiation-induced heart disease: a review of classification, mechanism and prevention. *Int J Biol Sci.* 2019;15(10):2128-2138. [doi pubmed pmc](#)
- Raghunathan D, Khilji MI, Hassan SA, Yusuf SW. Radiation-Induced Cardiovascular Disease. *Curr Atheroscler Rep.* 2017;19(5):22. [doi pubmed](#)
- Schultz-Hector S. Radiation-induced heart disease: review of experimental data on dose response and pathogenesis. *Int J Radiat Biol.* 1992;61(2):149-160. [doi pubmed](#)
- Stewart FA, Hoving S, Russell NS. Vascular damage as an underlying mechanism of cardiac and cerebral toxicity in irradiated cancer patients. *Radiat Res.* 2010;174(6):865-869. [doi pubmed](#)
- Erven K, Florian A, Slagmolen P, Sweldens C, Jurcut R, Wildiers H, Voigt JU, et al. Subclinical cardiotoxicity detected by strain rate imaging up to 14 months after breast radiation therapy. *Int J Radiat Oncol Biol Phys.*

- 2013;85(5):1172-1178. [doi pubmed](#)
15. Xu T, Meng QH, Gilchrist SC, Lin SH, Lin R, Xu T, Milgrom SA, et al. Assessment of prognostic value of high-sensitivity cardiac troponin t for early prediction of chemoradiation therapy-induced cardiotoxicity in patients with non-small cell lung cancer: a secondary analysis of a prospective randomized trial. *Int J Radiat Oncol Biol Phys.* 2021;111(4):907-916. [doi pubmed pmc](#)
 16. Fan LL, Luo YK, Xu JH, He L, Wang J, Du XB. A dosimetry study precisely outlining the heart substructure of left breast cancer patients using intensity-modulated radiation therapy. *J Appl Clin Med Phys.* 2014;15(5):4624. [doi pubmed pmc](#)
 17. Tang S, Koh E, Delaney G, George A, Tran D, Otton J, et al. Quantification of cardiac subvolume dosimetry in breast cancer patients receiving tangential beam radiation therapy. *International Journal of Radiation Oncology Biology Physics.* 2017;99(2):E32. [doi](#)
 18. Tang S, Otton J, Holloway L, Delaney GP, Liney G, George A, Jameson M, et al. Quantification of cardiac subvolume dosimetry using a 17 segment model of the left ventricle in breast cancer patients receiving tangential beam radiotherapy. *Radiother Oncol.* 2019;132:257-265. [doi pubmed](#)
 19. Eldredge-Hindy HB, Duffy D, Yamoah K, Simone NL, Skowronski J, Dicker AP, Anne PR. Modeled risk of ischemic heart disease following left breast irradiation with deep inspiration breath hold. *Pract Radiat Oncol.* 2015;5(3):162-168. [doi pubmed](#)
 20. Korreman SS, Pedersen AN, Aarup LR, Notttrup TJ, Specht L, Nystrom H. Reduction of cardiac and pulmonary complication probabilities after breathing adapted radiotherapy for breast cancer. *Int J Radiat Oncol Biol Phys.* 2006;65(5):1375-1380. [doi pubmed](#)
 21. Smyth LM, Knight KA, Aarons YK, Wasiaik J. The cardiac dose-sparing benefits of deep inspiration breath-hold in left breast irradiation: a systematic review. *J Med Radiat Sci.* 2015;62(1):66-73. [doi pubmed pmc](#)
 22. Hayden AJ, Rains M, Tiver K. Deep inspiration breath hold technique reduces heart dose from radiotherapy for left-sided breast cancer. *J Med Imaging Radiat Oncol.* 2012;56(4):464-472. [doi pubmed](#)
 23. Shah C, Badiyan S, Berry S, Khan AJ, Goyal S, Schulte K, Nanavati A, et al. Cardiac dose sparing and avoidance techniques in breast cancer radiotherapy. *Radiother Oncol.* 2014;112(1):9-16. [doi pubmed](#)
 24. Latty D, Stuart KE, Wang W, Ahern V. Review of deep inspiration breath-hold techniques for the treatment of breast cancer. *J Med Radiat Sci.* 2015;62(1):74-81. [doi pubmed pmc](#)
 25. Sripathi LK, Ahlawat P, Simson DK, Khadanga CR, Kamarsu L, Surana SK, Arasu K, et al. Cardiac dose reduction with deep-inspiratory breath hold technique of radiotherapy for left-sided breast cancer. *J Med Phys.* 2017;42(3):123-127. [doi pubmed pmc](#)
 26. Stewart JR, Fajardo LF. Radiation-induced heart disease: an update. *Prog Cardiovasc Dis.* 1984;27(3):173-194. [doi pubmed](#)
 27. Wang K, Pearlstein KA, Patchett ND, Deal AM, Mavroidis P, Jensen BC, Lipner MB, et al. Heart dosimetric analysis of three types of cardiac toxicity in patients treated on dose-escalation trials for Stage III non-small-cell lung cancer. *Radiother Oncol.* 2017;125(2):293-300. [doi pubmed pmc](#)
 28. Duma MN, Herr AC, Borm KJ, Trott KR, Molls M, Oechsner M, Combs SE. Tangential field radiotherapy for breast cancer-the dose to the heart and heart subvolumes: what structures must be contoured in future clinical trials? *Front Oncol.* 2017;7:130. [doi pubmed pmc](#)
 29. Evans ES, Prosnitz RG, Yu X, Zhou SM, Hollis DR, Wong TZ, Light KL, et al. Impact of patient-specific factors, irradiated left ventricular volume, and treatment set-up errors on the development of myocardial perfusion defects after radiation therapy for left-sided breast cancer. *Int J Radiat Oncol Biol Phys.* 2006;66(4):1125-1134. [doi pubmed](#)
 30. Stam B, Peulen H, Guckenberger M, Mantel F, Hope A, Werner-Wasik M, Belderbos J, et al. Dose to heart substructures is associated with non-cancer death after SBRT in stage I-II NSCLC patients. *Radiother Oncol.* 2017;123(3):370-375. [doi pubmed](#)
 31. McWilliam A, Faivre-Finn C, Kennedy J, Kershaw L, van Herk M. Data mining identifies the base of the heart as a dose-sensitive region affecting survival in lung cancer patients. *International Journal of Radiation Oncology Biology Physics.* 2016;96(2):S48-S49. [doi](#)
 32. Feng M, Moran JM, Koelling T, Chughtai A, Chan JL, Freedman L, Hayman JA, et al. Development and validation of a heart atlas to study cardiac exposure to radiation following treatment for breast cancer. *Int J Radiat Oncol Biol Phys.* 2011;79(1):10-18. [doi pubmed pmc](#)
 33. Howell RM, Scarboro SB, Kry SF, Yaldo DZ. Accuracy of out-of-field dose calculations by a commercial treatment planning system. *Phys Med Biol.* 2010;55(23):6999-7008. [doi pubmed pmc](#)
 34. Guzha L, Mendenhall NP, Morris CG, Flampouri S, Hoppe BS. Evaluating cardiac biomarkers after chemotherapy and proton therapy for mediastinal Hodgkin lymphoma. *Int J Part Ther.* 2017;4(2):35-38. [doi pubmed pmc](#)
 35. Yeung R, Conroy L, Long K, Walrath D, Li H, Smith W, Hudson A, et al. Cardiac dose reduction with deep inspiration breath hold for left-sided breast cancer radiotherapy patients with and without regional nodal irradiation. *Radiat Oncol.* 2015;10:200. [doi pubmed pmc](#)
 36. Brady LW, Heilmann H, Molls M. New technologies in radiation oncology. Springer; 2006.